ORGANOMETALLICS

Article

pubs.acs.org/Organometallics

Kinetics and Mechanistic Insights into the Acetate-Assisted Dimerization of Terminal Alkynes under Ruthenium- and Acid-Promoted (RAP) Catalysis

Riccardo Salvio,[†] Francisco Juliá-Hernández,[†] Luca Pisciottani,[†] Rafael Mendoza-Meroño,[‡] Santiago García-Granda,[‡] and Mauro Bassetti*[,†]

[†]Istituto di Metodologie Chimiche (IMC) del Consiglio Nazionale delle Ricerche (CNR), Sezione Meccanismi di Reazione, and Dipartimento di Chimica, Sapienza Università di Roma, P.le A. Moro 5, I-00185 Roma, Italy

[‡]Departamento de Química Física y Analítica, Facultad de Química, Universidad de Oviedo, E-33006 Oviedo, Spain

Supporting Information

ABSTRACT: The mechanism of the dimerization of terminal aryl alkynes promoted by [{RuCl(μ-Cl)(η⁶-*p*-cymene)}₂](**1**)/AcOH, under cooperative transition metal/Brønsted acid catalysis, has been investigated with regard to (i) the activation of the dinuclear ruthenium complex and (ii) the catalytic formation of the *trans*-1,4-diaryl-1,3-enyne products, by a detailed kinetic investigation of both processes. Complex **1** is subject to a slow solvolytic process in neat acetic acid or is transformed rapidly in the presence of sodium acetate to form the monomeric ruthenium(II) acetato complex [RuCl(η⁶-*p*-cymene)(OAc)]. The latter is the active catalytic species promoting the alkyne dimerization process, via initial π-alkyne coordination and intramolecular C−H abstraction by the acetate ligand, as key steps of the catalytic cycle. The presence of additive acetate salts allows for the reaction to proceed at room temperature with short reaction times and high *trans*/*cis* stereoselectivity, thus rendering this catalytic system among the most active and selective procedures for the dimerization of terminal alkynes in a protic medium. The linear coupling of three molecules of phenylacetylene affords an organometallic ruthenium complex featuring a butenynyl ligand which has been characterized by X-ray crystallography.

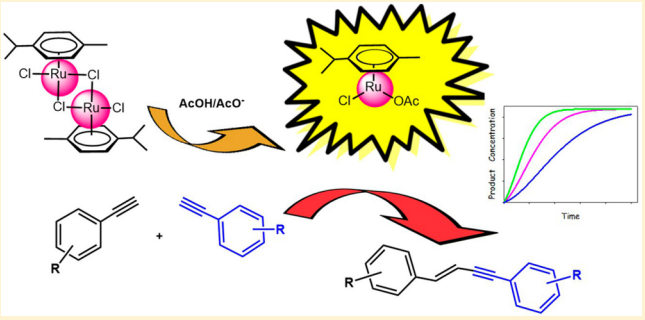

INTRODUCTION

The dimerization of terminal alkynes promoted by transition-metal complexes has gained increasing interest as a potential synthetic tool for the preparation of conjugated enynes.[1] In the past decade the intrinsic limits of the reaction due to the variety of possible chemo-, regio-, and stereoisomeric products have been progressively overcome with the development of selective catalytic systems.[2] As a result, synthetic applications of the process have also appeared, in particular in the field of materials with optoelectronic properties.[3]

Ruthenium(II) complexes have emerged among the most active and selective catalysts,[1,4] allowing for reactions even in protic and aqueous media.[5] In this context we previously reported that the complex [{RuCl(μ-Cl)(η⁶-*p*-cymene)}₂] (**1**) dissolved in acetic acid generates in situ a catalytic system able to promote the dimerization of terminal aromatic alkynes at room temperature, thus affording the coupling products *trans*-ArCH═CHC≡CAr with high selectivity of the double bond.[6] Under analogous conditions, aromatic diynes can be transformed into polyaddition oligomers or polymers, as fluorescent materials soluble in organic solvents (Chart 1).[3a,7] The robustness of the catalytic system based on **1** in AcOH allows for the C−C coupling process to be performed in one pot after desylilation of (trimethylsilyl)arylacetylene substrates ($Me_3SiC{\equiv}CAr$) under either basic or acidic conditions.[8] Moreover, the hexamethylbenzene ruthenium dimer [{RuCl(μ-Cl)(η⁶-C_6Me_6)}₂] (**2**) promotes the synthesis of enynes with high efficiency and trans selectivity in the mixed aqueous medium AcOH/H_2O.[9]

Interestingly, during the course of these studies it was observed that the presence of acetate salts in the reaction mixture provided significant rate enhancements.[8,9] This evidence might account for the generation of acetate ruthenium complexes, which are presumably involved as catalytic

Chart 1. Dimerization of Terminal Alkynes Promoted by [{RuCl(μ-Cl)(η⁶-*p*-cymene)}₂] (1) in Acetic Acid

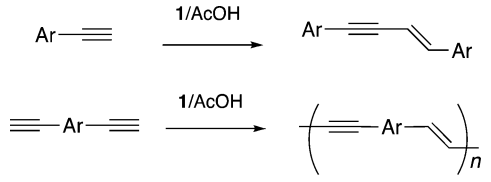

Received: July 31, 2017
Published: September 21, 2017

DOI: 10.1021/acs.organomet.7b00583
Organometallics 2017, 36, 3830−3840

intermediates facilitating the coupling process. Similarly, in the field of palladium- or ruthenium-catalyzed arylation or alkylation of substituted arenes, a base-assisted deprotonation of the C−H bond has been recognized to be crucial in the formation of active cyclometalated intermediates.[10] Relevant synthetic applications, which have recently been extended to the annulation of internal alkynes,[11] rely precisely on the carboxylate ligand acting as an intramolecular base for the C−H deprotonation step, resulting in a variety of C−C and C−Het coupling products. Regarding terminal alkynes, the stoichiometric π-alkyne to acetylide and then vinylidene transformations in the coordination sphere of acetato ruthenium(II) complexes have been documented,[12] whereas specific evidence of carboxylate assistance to the dimerization reaction has been reported for a palladium catalyst.[13] In the latter case, it was found that the carboxylate anion plays an important role in switching the dimerization from head to head to head to tail coupling.

In light of the intriguing effect of acetate salts in the dimerization of terminal alkynes promoted by **1**/AcOH and of related processes of interest in the area of C−H functionalization, we wished to understand the effect of the carboxylate ligand on a more sophisticated level by investigating both the formation of the catalytic species from the precursor complex **1** and the catalytic alkyne dimerization. Accordingly, we have carried out a kinetic study for both reaction phases. The kinetic experiments and analysis have allowed us to draw a detailed mechanistic picture of the catalytic system in action, including the solvolysis of the ruthenium dimer into monomeric acetato species and the effect of the alkyne structure and of acetate additives in the C−C coupling process. The formation and X-ray structural analysis of a complex involving a trimeric alkyne ligand are also described.

RESULTS AND DISCUSSION

Activation Stage. The complex $[\{RuCl(\mu\text{-}Cl)(\eta^6\text{-}p\text{-cymene})\}_2]$ is electronically and coordinatively saturated and hence a poor candidate for productive interaction with an organic substrate. The transformation into a monomeric species can therefore be regarded as crucial for the expression of catalytic activity and can be postulated according to the equilibrium outlined in eq 1, derived from the interaction of **1** with the protic solvent. Along this line, we have investigated the behavior of complex **1** by UV−vis spectroscopy. The spectrum (Figure S1 in the Supporting Information) of a freshly prepared solution of complex **1** in AcOH (λ_{max} 340 and 438 nm; ε_{438} = 1706 M^{-1} cm^{-1}) is similar to the spectrum in dichloromethane (λ_{max} 268, 338, 448 nm; ε_{448} = 2432 M^{-1} cm^{-1}), the only appreciable difference being a small red shift of the absorption band in the visible region ($\Delta\lambda$ = 10 nm). Since ligand exchange phenomena with solvent molecules or dissociative processes in dichloromethane are unlikely, it can be deduced that complex **1** in acetic acid remains essentially in its dinuclear form.

$$[\{RuCl(\mu\text{-}Cl)(\eta^6\text{-}p\text{-cymene})\}_2]_{\mathbf{1}} + 2AcOH \rightleftarrows 2[RuCl(OAc)(\eta^6\text{-}p\text{-cymene})]_{\mathbf{3}} + 2HCl \quad (1)$$

However, when the same solution was monitored over a time scale of several hours, the spectrum of **1** changed slightly, exhibiting an appreciable decrease of absorbance of the maximum at 340 nm, along with a very moderate increase at 310 nm, thus indicating that **1** is subject to a slow transformation by interaction with acetic acid. In search for evidence that the small changes observed may be related to the formation of complex **3** (eq 1), the spectrum of **1** was also recorded in the presence of sodium acetate, at room temperature. In this case, the spectral features of **1** exhibited a dramatic change, indicating the formation of a new species. Figure 1 shows the spectrum of the ruthenium dimer in acetic

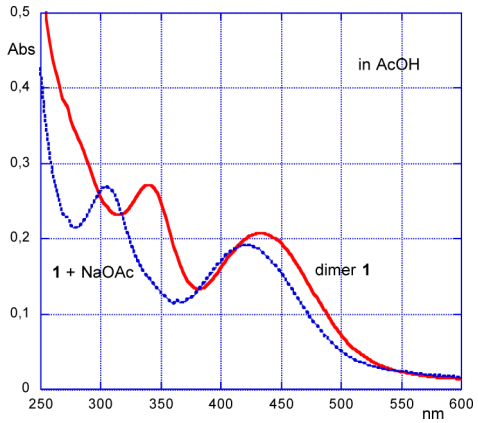

Figure 1. UV−visible spectra of complex $[\{RuCl(\mu\text{-}Cl)(\eta^6\text{-}p\text{-cymene})\}_2]$ (**1**; 0.106 mM, red trace) in acetic acid and of the same solution after addition of sodium acetate (10.6 mM, blue trace), at 20 °C.

acid (red trace) and that obtained upon addition of sodium acetate (100 equiv, blue trace), shortly after mixing. The resulting spectrum matched with that of an authentic sample of the acetate complex **3**, characterized by red shifts of the absorption bands in the visible region (λ_{max} 306 and 417 nm; ε_{417} = 1180 M^{-1} cm^{-1}) with respect to those of the dimer **1**. Since further changes were not observed upon monitoring the solution over a period of a few hours, the reaction of complex **1** with sodium acetate under the above conditions can be regarded as quantitative, as outlined in eq 2. The transformation is characterized by the disappearance of the band at 340 nm of **1** and a moderate absorbance increase at 310 nm, in line with the small changes observed for the solution of **1** in neat AcOH.

$$[\{RuCl(\mu\text{-}Cl)(\eta^6\text{-}p\text{-cymene})\}_2]_{\mathbf{1}} + 2NaOAc \rightarrow 2[RuCl(OAc)(\eta^6\text{-}p\text{-cymene})]_{\mathbf{3}} + 2NaCl \quad (2)$$

On the other hand, it is already known that arene ruthenium(II) dichloride dimers are transformed into carboxylate complexes when they are heated in a solution of acetic anhydride and carboxylic acid[14] or by reaction with metal carboxylates. In particular, $[RuCl(\kappa^2\text{-}OAc)(\eta^6\text{-}p\text{-cymene})]$ (**3**) was prepared from the reaction of **1** with sodium acetate in dichloromethane or in methanol at ambient temperature.[15]

Since the UV−vis experiments indicate that the transformation of **1** into the monomeric species **3** occurs rapidly in the presence of an acetate salt (eq 2) or occurs at a much lower rate in acetic acid only (eq 1), we proceeded to obtain rate data for the reaction in both cases. As the alkyne dimerization promoted by **1** proceeds in either the absence or presence of the acetate cocatalyst, any derived information can also be of interest for the C−C coupling process itself.

DOI: 10.1021/acs.organomet.7b00583
Organometallics 2017, 36, 3830−3840

The reaction in neat AcOH was monitored at different temperatures upon following the decrease of absorbance at 340 nm; values of observed rate constants (k_{obs}, s^{-1}) were obtained using the method of the initial rates from data obtained in the range from 0 to 15% reaction and are reported in Table 1.

Table 1. First-Order Rate Constants for the Conversion of Complex 1 (Eq 1) in Neat AcOH[a]

entry	T (°C)	k_{obs} (s^{-1})
1	29.2	1.2×10^{-6}
2	41.6	4.5×10^{-6}
3	53.8	2.3×10^{-5}
4	63.8	7.5×10^{-5}

[a] [**1**] = 1.0×10^{-4} M. λ = 340 nm.

A least-squares fitting procedure of these rate data according to the Eyring equation affords the activation parameters $\Delta H^{\ddagger}$ = 25.3(±0.4) kcal mol^{-1} and $\Delta S^{\ddagger}$ = −2.4(±1.1) cal mol^{-1} K^{-1} (Figure S15 in the Supporting Information).

The rate of formation of complex **3** from **1** was then investigated in the presence of different concentrations of NaOAc. The changes of absorbance at 340 and/or 450 nm were followed using a stopped-flow apparatus for the measurements at [NaOAc] > 0.5 mM, under pseudo-first-order conditions, and by the initial rates method for the measurements in the lower concentration range. The kinetic analyses afforded the values of observed rate constants (k_{obs}, s^{-1}) reported in Table 2.

Table 2. Observed Rate Constants for the Reaction of Complex 1 with NaOAc in Acetic Acid at 25 °C

entry	[NaOAc] (M)	[Bu_4NCl] (mol L^{-1})	k_{obs} (s^{-1})[a]
1	2.0×10^{-5}		0.045[b]
2	1.0×10^{-4}		0.17[b]
3	5.5×10^{-4}		0.42[c]
4	1.1×10^{-3}		0.38[c]
5	1.1×10^{-2}		0.44[c]
6	5.5×10^{-2}		0.42[c]
7	2.0×10^{-5}	0.25	0.039[b]
8	2.0×10^{-5}	0.50	0.028[b]
9	2.0×10^{-5}	0.75	0.021[b]
10	2.0×10^{-5}	1.00	0.012[b]

[a] ±15%. The experimental uncertainty is also shown in Figure 2 as error bars. [b] Values obtained by the initial rates method. [c] Values obtained under pseudo-first-order conditions ([**1**] = (0.1−1.0) × 10^{-4} M).

Comparison of the data in Tables 1 and 2 confirms the dramatic rate difference for the reaction in neat acetic acid or in the presence of acetate. In the latter case, the k_{obs} values are dependent on acetate in the lower concentration range while they tend to level off toward an asymptotic value for [NaOAc] ≥ 0.5 mM, as shown in the plot of Figure 2. This evidence seems to exclude a rate-determining attack of AcO^- to the ruthenium dimer, which should exhibit linear dependence on concentration of the nucleophile. Since ligand and in particular chloride dissociation in polar solvents represents a key step in both stoichiometric or catalytic reactions of octahedral ruthenium(II) complexes, a mechanism based on solvent-assisted ruthenium−chloride bond breaking in **1** with release of Cl^- and formation of the solvated cationic intermediate [**1** − Cl^-] ($\mathbf{1}^+$) is a likely pathway (eq 3). The rapid attack by acetate or by AcOH to $\mathbf{1}^+$ and the subsequent breakdown of an acetato complex ($\mathbf{1}^+AcO^-$) yield monomeric species of type **3** (eqs 4 and 5; L = η^6-*p*-cymene).

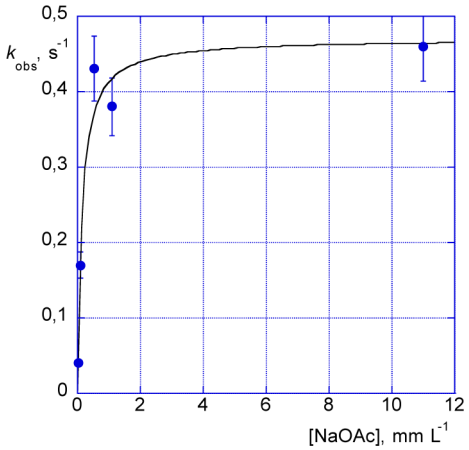

Figure 2. Observed rate constants (±15%) vs concentration of sodium acetate in the conversion of **1** into **3**. The data points are from Table 2, and the curved line represents the best fit with eq 6.

$$\mathbf{1}\cdot(AcOH)_n \underset{k_{-1}}{\overset{k_1}{\rightleftarrows}} (\mathbf{1}^+)\cdot(AcOH)_n + Cl^- \quad (3)$$

$$\mathbf{1}^+ + AcO^- \xrightarrow{k_2} \mathbf{1}^+AcO^- \xrightarrow[-Cl]{AcO^-} 2[RuCl(OAc)L] \quad (4)$$

$$\mathbf{1}^+ + AcOH \xrightarrow[-H^+]{k_2'} \mathbf{1}^+AcO^- \xrightarrow[-HCl]{AcOH} 2[RuCl(OAc)L] \quad (5)$$

By assuming formation of the solvated intermediate $\mathbf{1}^+$ under steady-state conditions, the derived rate expression of this mechanism is given by eq 6.

$$k_{obs} = \frac{k_1 k_2 [AcO^-]}{k_{-1}[Cl^-] + k_2[AcO^-]} \quad (6)$$

Accordingly, the k_{obs} values exhibit dependence on $[AcO^-]$ in the lower concentration range (Figure 2), where the terms $k_{-1}[Cl^-]$ and $k_2[AcO^-]$ may be comparable in size, whereas the rate expression reduces to $k_{obs} = k_1$ under the conditions that $k_{-1}[Cl^-] \ll k_2[AcO^-]$, in agreement with the observed saturation behavior at high $[AcO^-]$. A large value of k_2/k_{-1} is also a reasonable expectation, since the competition between acetate and chloride for the intermediate should favor the more basic species. The best fit with a nonlinear least-squares procedure of the data points from Table 2 to eq 6 gives the limiting value of k_1 = 0.47 ± 0.06 s^{-1}, which should represent the rate constant of chloride dissociation from complex **1**. The linear version of eq 6 yields the interpolated value of k_1 = 0.55 ± 0.1 s^{-1} (eq 7), in reasonable agreement with the nonlinear best fit analysis (Figure S13 in the Supporting Information).

$$\frac{1}{k_{obs}} = \frac{k_{-1}[Cl^-]}{k_1 k_2 [AcO^-]} + \frac{1}{k_1} \quad (7)$$

One alternative to the purely dissociative mechanism of eqs 3 and 4 that is compatible with the rate data of Table 2 can be described in terms of a rapid pre-equilibrium between complex **1** and acetate (K, eq 8) to give the outer-sphere complex **1**·AcO^-. Exchange of chloride with acetate in the rate-

DOI: 10.1021/acs.organomet.7b00583
Organometallics 2017, 36, 3830−3840

determining step (k_2, eq 9) is then followed by rapid evolution into monomeric complexes.[16]

$$\mathbf{1} + \mathrm{AcO^-} \overset{K}{\rightleftarrows} (\mathbf{1}\cdot\mathrm{AcO^-}) \quad (8)$$

$$(\mathbf{1}\cdot\mathrm{AcO^-}) \overset{k_2}{\rightarrow} \mathbf{1}^+\mathrm{AcO^-} + \mathrm{Cl^-} \quad (9)$$

Equation 10 represents the derived expression for this mechanism, and it is similar to the Michaelis–Menten equation.

$$k_{obs} = \frac{Kk_2[\mathrm{AcO^-}]}{1 + K[\mathrm{AcO^-}]} \quad (10)$$

In both mechanisms, chloride dissociation is involved in the rate-determining step, either directly from dimer **1** to yield the cationic species $\mathbf{1}^+$ (eq 3) or within the molecular complex ($\mathbf{1}\cdot\mathrm{AcO^-}$) to give $\mathbf{1}^+\mathrm{AcO^-}$ (eq 9). In octahedral ruthenium(II) complexes, chloride dissociation is commonly a key step in both stoichiometric or catalytic reactions,[17] and chloride substitution reactions often proceed by dissociative mechanisms.[18]

Though the mechanisms depicted by eqs 6 and 10 are indistinguishable on the basis of the kinetic data in Table 2 (entries 1–6), additional experiments performed at constant [NaOAc] in the presence of tetrabutylammonium chloride clearly indicate a modest rate suppression as a function of [Bu_4NCl] (Table 2, entries 1 and 7–10, and Figure S14 in the Supporting Information). This evidence suggests that an excess of chloride ions in solution may influence and shift the equilibrium in eq 3 by a mass balance effect, thus reducing the concentration of intermediate $\mathbf{1}^+$. The analysis of these data in terms of eq 7 and the corresponding linear plot of $1/k_{obs}$ vs [Bu_4NCl] affords the value $k_1 = 0.54 \pm 1\ s^{-1}$ from the intercept and the ratio $k_{-1}/k_2 = [5.0(\pm1.5)] \times 10^{-4}$ from the slope, in agreement with the previous considerations.

The mechanism for the reaction in neat acetic acid can also be discussed in similar terms, but with the presence of the solvent molecules instead of acetate ions, according to eqs 3 and 5. The value of the activation entropy close to 0 is consistent with a rate-limiting dissociative step (eq 3) being accompanied by extensive solvation of the derived ions. A unifying picture of the solvolysis of complex **1** is represented in Scheme 1.

Dimerization Reaction of Arylacetylenes Promoted by Complex 1. The dimerization of phenylacetylene catalyzed by **1** was followed in situ by ^{1}H NMR using CD_3CO_2H as solvent at different catalyst loads and temperatures. Reaction profiles for the transformation of **4a** at 29 °C upon varying [**1**] are shown in Figure 3. Relevant data obtained from these experiments, including yield of *trans*-enyne **5a** and stereoisomeric *trans*/*cis* ratio, are reported in Table 3. Appreciable amounts of the *gem* isomer were not observed under these conditions. The best compromise between activity and catalyst load was obtained with 4 mol % of **1**, giving rise to a near 80% calculated yield of enyne, while the reaction was sluggish with 2 mol % and no useful changes were found using 8 mol % of the complex (Table 3, entries 1–3). Yields of enyne product and stereoselectivity (**5a**:**5b** = 97:3) did not change appreciably at different temperatures.

When the run was performed in CD_3CO_2D, the conversion of phenylacetylene was accompanied by concomitant H–D exchange in the terminal triple bond and the enyne product was only observed in the ^{1}H NMR spectrum as traces of PhC≡CCH=CDPh. The major component PhC≡CCD=CDPh (**5a**-d_2, 38%) was detected along with PhC≡CD (**4a**-d_1, 43%) by GC-MS analysis, upon workup of the reaction mixture (Table 3, entry 4). Such a decrease in activity can be related to

Scheme 1. Mechanism of Acetolysis of Complex 1

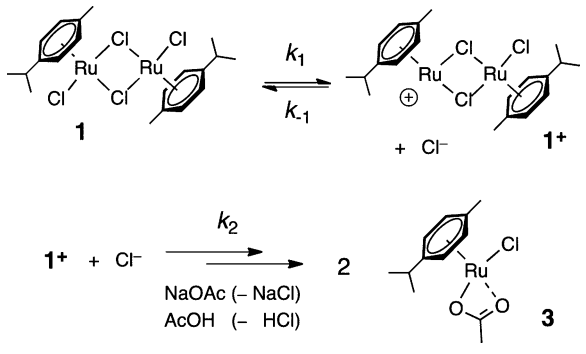

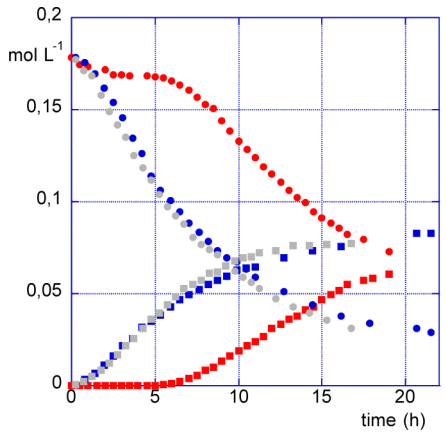

Figure 3. Dimerization of phenylacetylene (**4a**, circle) followed by ^{1}H NMR in CD_3CO_2H, yielding *trans*-PhCH=CHC≡CPh (**5a**, square) in the presence of [{RuCl(μ-Cl)(η^6-*p*-cymene)}$_2$]. Conditions: amount of **1** (mol %) 8.4 (gray), 4.4 (blue), 2.0 (red); 29.2 °C.

Table 3. Dimerization of Phenylacetylene in the Presence of [{RuCl(μ-Cl)(η^6-*p*-cymene)}$_2$] in CD_3CO_2H[a]

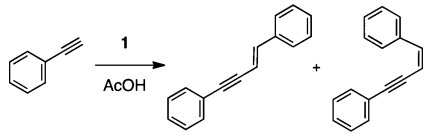

4a 5a 5b

entry	**1** (%)	T (°C)	**5a**[b,c] (%)	k_{cat_3}[d] ($M^{-1}\ s^{-1}$)	k_{cat_1}[d] (s^{-1})
1	2.0	29.2	36	1.5×10^{-2}	9.4×10^{-4}
2	4.1	29.2	83	1.6×10^{-2}	1.0×10^{-3}
3	8.5	29.2	76	1.9×10^{-2}	1.3×10^{-3}
4[e]	4.3	29.2	38[f]		
5	4.4	41.6	82	9.4×10^{-2}	2.3×10^{-3}
6	4.1	53.8	83	0.13	6.0×10^{-3}
7	4.4	63.8	85	0.31	

[a] [**4a**] = 0.180 mol L^{-1}. [b] Estimated percent conversion of **4a** to **5a** on the basis of ^{1}H NMR data (±6%). [c] **5a**:**5b** = 97:3. [d] ±15%. [e] In CD_3CO_2D. [f] Determined by GC-MS.

DOI: 10.1021/acs.organomet.7b00583
Organometallics 2017, 36, 3830–3840

the different proton-donor strengths of acetic acid and acetic acid-d_1, the pK_a value of the medium changing from 4.74 to 5.35,[19] and agrees with the presence of proton transfer steps in the catalytic cycle. In this respect, the role of the proton donor from either the terminal alkyne or the medium is well-known for alkyne dimerization reactions, including effects on the *cis*/*trans* stereoselectivity or the switch to a different process.[20]

Inspection of the plots in Figure 3 evidence that the disappearance of the substrate (**4a**, ○) and the formation of the enyne *trans*-PhCH═CHC≡C-Ph (**5a**, □) follow a sigmoidal pattern, suggesting that the dimerization reaction is slower in the early stages due to the buildup of active catalytic species. By taking into account the results described in the previous section, it seems reasonable to assume that the observed activation stage is the consequence of the slow formation of species of type [RuCl(OAc))(η^6-*p*-cymene)] (**3**) from the chloride complex **1**.

On these bases, we have performed a detailed kinetic analysis of the process initiated by the dimer **1**, with the intention to recognize different contributions to the overall reaction profile and, ultimately, express the role of the various components. The formation of **5a** from the experiments performed at 29, 42, and 54 °C in the presence of 4.4 mol % of **1** is represented graphically in the concentration/time plots of Figure 4. As a

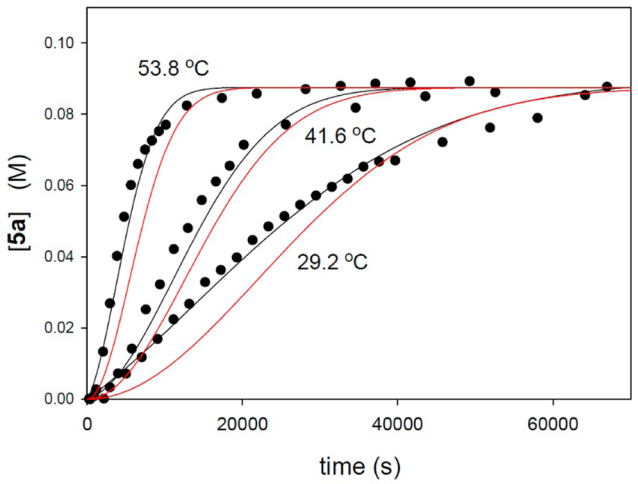

Figure 4. Dimerization of phenylacetylene **4a** in the presence of **1** (4.4%) in AcOH at different temperatures (29.2, 41.6, 53.8 °C). The solid lines represent the fitting of the experimental data points to eq 16 or 18 as red or black lines, respectively.

first approximation, the process can be analyzed in terms of generation of the mononuclear species **3** from complex **1** (*activation stage*, eq 11) and conversion of the substrate into the product upon catalysis by **3** (*dimerization*, eq 12).

$$\text{complex } \mathbf{1} \xrightarrow{k_s} 2 \text{ complex } \mathbf{3} \tag{11}$$

$$\mathbf{4a}(\text{alkyne}) \xrightarrow{k_{cat\_3}} 1/2\ \mathbf{5a} \tag{12}$$

The two reactions are assumed to follow the kinetic expressions represented in eqs 13 and 14, where k_s is the rate constant for the solvolysis of complex **1** to yield **3** and k_{cat_3} is the rate constant for the reaction catalyzed by the active species **3**. The rate equation (14) implies that the reaction is first order in alkyne and first order in complex **3**, corresponding to pseudo-first-order conditions upon assumption that [**3**] remains constant during the catalytic cycle. On the other hand, a second-order rate dependence on alkyne concentration, and hence the use of a quadratic term ([alkyne]^2) in eq 14, is not compatible with the observed kinetic plots, which tend to level off to saturation values of the enyne concentration, as is typical of first-order reactions. The substitution of [**3**] in the integrated expression resulting from eq 14 yields eq 15, where $[\mathbf{1}]_0$ is the initial concentration of the ruthenium dimer **1**.

$$\frac{d[\mathbf{3}]}{dt} = 2k_s[\mathbf{1}] \tag{13}$$

$$\frac{d[\mathbf{5a}]}{dt} = k_{cat\_3}[\mathbf{3}][\text{alkyne}] \tag{14}$$

$$-\frac{d[\mathbf{4a}]}{dt} = 2k_{cat\_3}[\mathbf{1}]_0(1 - e^{-k_s t})[\mathbf{4a}] \tag{15}$$

Rearrangement and integration of eq 15 affords eq 16.

$$[\mathbf{5a}] = \frac{[\mathbf{4a}]_0}{2}\left(1 - e^{2k_{cat\_3}[\mathbf{1}]_0(1/k_s - t - 1/k_s e^{-k_s t})}\right) \tag{16}$$

The values of k_s are the observed rate constants (k_{obs}) which were obtained independently at the same temperatures (Table 1) and were used as known quantities to fit the kinetic data by a nonlinear least-squares procedure. Fitting of the data points with this equation was not satisfactory (Figure 4, red lines). Upon taking into consideration various options, we have tested the possibility that the original complex **1** may also give a minor contribution to the catalysis and so have extended eq 16 to include a rate constant for the alkyne dimerization catalyzed by the dinuclear species (k_{cat_1}). Integration of the resulting equation (17), which can be considered a more general expression of eq 16, gives eq 18.

$$-\frac{d[\mathbf{4a}]}{dt} = 2k_{cat\_3}[\mathbf{1}]_0(1 - e^{-k_s t})[\mathbf{4a}] + k_{cat\_1}[\mathbf{1}]_0 e^{-k_s t}[\mathbf{4a}] \tag{17}$$

$$[\mathbf{5a}] = \frac{[\mathbf{4a}]_0}{2}\left(1 - e^{2k_{cat\_3}[\mathbf{1}]_0(1/k_s - t - 1/k_s e^{-k_s t}) + k_{cat\_1}[\mathbf{1}]_0(e^{-k_s t})}\right) \tag{18}$$

In this case, k_{cat_1} and k_{cat_3} were treated as the only adjustable parameters. The least-squares procedures gave the fittings shown in Figure 4 in black, and the corresponding values of the best-fit parameters are given in Table 3.

Equation 18 expresses that the contribution of complex **3** becomes increasingly larger at longer reaction times due to the buildup of this species at the expense of complex **1**. It is worth mentioning that the data points for either formation of the enyne or disappearance of the alkyne, upon exclusion of those at initial ~15% reaction, give acceptable fits with the first-order rate equation and, accordingly, linear plots of ln[**4a**] vs time (Figures S18 and S20 in the Supporting Information).

This situation, in agreement with eq 14, indicates, unexpectedly, that the reaction is first order with respect to the terminal alkyne, instead of second order, in spite of the fact that the overall reaction involves 2 mol of **4a** (this is confirmed by consistent deviation from linearity in plots of [**4a**]$^{-1}$ vs time). The dimerization of phenylacetylene has been indeed found to be second order in alkyne when it is catalyzed by either a cationic tris(μ-hydroxo)diruthenium(II) complex[4a] or by a (NHC)platinum(0) complex.[2a] The only reasonable explanation of this experimental evidence in the catalysis by **1**/

DOI: 10.1021/acs.organomet.7b00583
Organometallics 2017, 36, 3830−3840

AcOH is that only one alkyne molecule is involved in the rate-determining step (rds) and that the other alkyne partner enters the catalytic cycle in subsequent rapid events. In fact, every substrate or reagent becoming part of a reaction sequence at a stage subsequent to the rds does not affect the rate of the reaction and gives no contribution to the overall reaction order. When the reaction was performed in the temperature range 29−64 °C, the Eyring plot derived from the rate constants for the disappearance of **4a** gave the following values of activation parameters $\Delta H^{\ddagger} = 14(\pm 3)$ kcal mol^{-1} and $\Delta S^{\ddagger} = -19(\pm 8)$ cal mol^{-1} K^{-1} (Figure S16 in the Supporting Information). The negative value of entropy of activation suggests an associative bimolecular rate-limiting step.

The dimerization promoted by **1** was then studied for arylacetylenes $RC_6H_4C{\equiv}CH$ featuring different ring substituents: i.e., R = *p*-OMe (**4b**), *m*-F (**4c**), *p*-CF_3 (**4d**), *p*-NO_2 (**4e**). The reactions were performed at 29 °C in CD_3CO_2H and followed by ^{1}H NMR, using the methodology and analytical treatment just described for **4a**. The conversion of each alkyne at approximately 4 half-lives of reaction, the corresponding yield of the *trans*-enyne product, the stereoisomeric ratio, and the k_{cat_3} values derived from fitting of the data points to eq 18 are reported in Table 4. The formation of the enyne is clearly

Table 4. Dimerization of $RC_6H_4C{\equiv}CH$ in the Presence of $[\{RuCl(\mu\text{-}Cl)(\eta^6\text{-}p\text{-cymene})\}_2]$ in CD_3CO_2H, Obtained by ^{1}H NMR[a]

entry	R	conversn of **4** (%) (**5** (%))[b]	*trans*:*cis*	k_{cat_3}[c] (10^5 M^{-1} s^{-1})
1	*p*-MeO	91 (91)	96:4	0.080
2	H	81 (79)	97:3	0.016
3	*m*-F	52 (48)	94:6	0.0085
4	*p*-CF_3	76 (68)	93:7	0.0020
5	*o*-CF_3	75 (12)[d]	>99:1	
6	*p*-NO_2	88 (−)[e]	96:4	

[a]Conditions: [alkyne] = 0.18 M; 1, 4.2 mol %, 29.2 °C. [b]Estimated percent conversion into **5** (*trans* + *cis*) on the basis of ^{1}H NMR data (±5%). [c]±15%. [d]Likely formation of polyacetylenes. [e]Precipitation of the product **5e** in the NMR tube hampered evaluation of conversion into enyne and rate data.

disfavored in the presence of an electron-withdrawing group (CF_3) in an ortho position (Table 4, entry 5). A plot of k_{cat_3} vs the Hammett σ values for the rest of the substituents, except NO_2, is shown in Figure 5.[21]

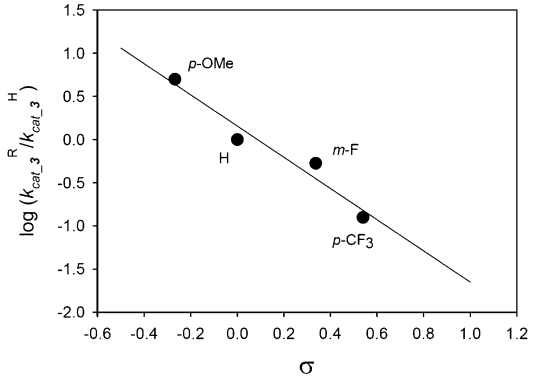

Figure 5. Hammett plot for the dimerization of aryl alkynes $RC_6H_4C{\equiv}CH$ in the presence of complex **1** in CD_3CO_2H at 29 °C.

The rate dependence on the substituent electronic effect corresponds to a reaction parameter $\rho = -1.8(\pm 0.3)$, indicating that increasing electron density of the triple bond favors the reaction.

Dimerization Reaction of Arylacetylenes Promoted by Complex 1/Metal Acetate. To find additional evidence for the activity of the ruthenium acetate complex as proposed in the previous section, an isolated sample of complex **3** was tested as a catalyst in the reaction of phenylacetylene. The time-dependent reaction profiles shown in Figure 6 highlight the

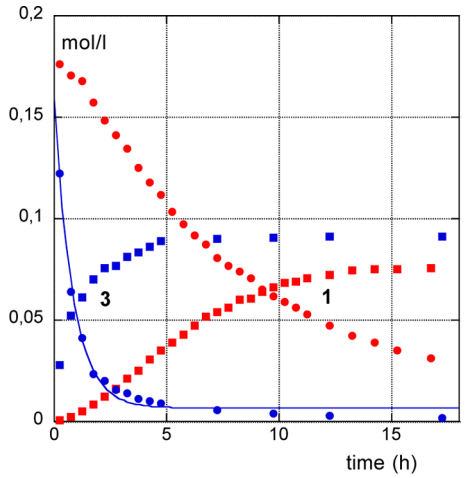

Figure 6. Dimerization of phenylacetylene (**4a**, circles) in CD_3CO_2H (29 °C), yielding *trans*-PhCH=CHC≡CPh (**5a**, squares) in the presence of complex $[\{RuCl(\mu\text{-}Cl)(\eta^6\text{-}p\text{-cymene})\}_2]$ (**1**, 8.4 mol %) or $[RuCl(OAc)(\eta^6\text{-}p\text{-cymene})]$ (**3**, 10.2 mol %).

remarkable rate difference observed upon using dimer **1** or the preformed acetate complex. In the latter case, both rapid conversion and absence of the induction period are evident effects. Treatment of the data points of [**5a**] vs time with the first-order rate equation gives a value of observed rate constant, $k_{obs} = 1.9 \times 10^{-4}$ s^{-1} corresponding to $k_{cat\_3} = 0.011$ M^{-1} s^{-1} (Table 5, entry 1), which is comparable with the best-fit parameters calculated from eq 18 for the reaction initiated by **1** (Table 3, entries 1−3).

The rapid transformation of the dimeric complex **1** into **3** upon addition of sodium acetate to the acetic acid solution and the remarkable catalytic activity of $[RuCl(OAc)(\eta^6\text{-}p\text{-cymene})]$ (**3**) suggest that the in situ generation of active catalytic species may represent a viable procedure based on the use of commercially available materials. Preliminary information in

Table 5. Dimerization of *p*-$RC_6H_4C{\equiv}CH$ in the Presence of $[\{RuCl(\mu\text{-}Cl)(\eta^6\text{-}p\text{-cymene})\}_2]$/MOAc in CD_3CO_2H

entry	alkyne (R)	**1** or **3** (mol %)	M	$\tau_{1/2}$ (m)	k_{cat_3}[a] (M^{-1} s^{-1})	*trans*:*cis*
1[b]	**4a** (H)	**3** (10)	none	60	0.011	>99:1
2[b]	**4a** (H)	**1** (8.4)	none	480	0.019	97:3
3[c]	**4a** (H)	**1** (2.7)	Li	94	0.012	98:2
4[c]	**4a** (H)	**1** (2.7)	Na	56	0.021	99:1
5[d]	**4d** (CF_3)	**1** (3.7)	Na	~6	*e*	>99:1
6[d]	**4d** (CF_3)	**1** (3.7)	none	148	0.0029	94:6

[a]±15%. [b][alkyne] = 0.18 mol L^{-1}, 29 °C. [c][alkyne] = 0.18 M, MOAc = 1 equiv, 27 °C, $k_{cat\_3} = k_{obs}/(2 \times [\mathbf{1}])$. [d]36 °C. [e]Poor kinetic fit.

DOI: 10.1021/acs.organomet.7b00583
Organometallics 2017, 36, 3830−3840

this respect was already obtained when the one-pot desilylation/dimerization procedure was developed[8] or when the dimerization of substituted arylalkynes (R = *p*-OMe, *p*-CHO, *p*-NO_2) catalyzed by the hexamethylbenzene complex **2** in the aqueous medium AcOH/H_2O was studied.[9]

We have tested the reaction in the presence of complex **1** and an acetate source for selected cases. In a typical procedure, an acetate salt was used in an equimolar amount with the substrate and so in large excess with respect to the ruthenium dimer, in order to ensure displacement of eq 2 to the right. For the analysis, the quantitative transformation of complex **1** into two molecules of **3** (eq 2) was assumed. Conditions and kinetic data of the experiments described in this section are reported in Table 5.

The kinetic profiles for the reaction of phenylacetylene in the presence of two different acetate salts are shown in Figure 7. It

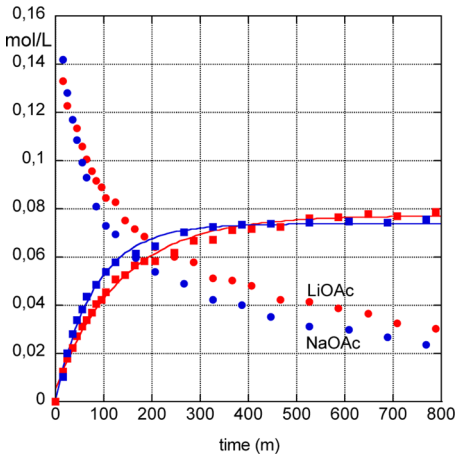

Figure 7. Dimerization of phenylacetylene (**4a**, circles) yielding *trans*-PhCH═CHC≡CPh (**5a**, squares) in the presence of complex (**1**, 2.7 mol %) and either lithium or sodium acetate (1 equiv), in CD_3CO_2H at 27 °C.

is remarkable that convenient reaction times are now accessible upon using less than 3 mol % of ruthenium dimer near room temperature, with *trans*/*cis* selectivity larger than 99%. The conversion into the enyne remains in the proximity of 80%, as in the case of the reaction initiated by complex **1** alone. Thus, improved catalytic activity affects the rate but not the reaction yield, as is implicit in the concept of catalysis. The plots in Figure 7 and the data in Table 5 indicate a moderate dependence of the reactivity on the nature of the countercation (Na vs Li), which is worthy of further analysis upon examination of different acetate salts.

The activity of the catalytic system **1**/NaOAc was also evaluated for the case of the deactivated alkyne **4d** (R = *p*-CF_3). The cocatalyst sodium acetate brings to completion the transformation into the corresponding *trans*-enyne in less than 1/2 h (calculated yield: 82% at 30 min), with approximately a 20-fold rate increase with respect to **1** alone and improved stereoselectivity (Figure 8 and Table 5, entries 5 and 6).

Whereas 1-octyne is inert in the **1**/AcOH mixture even at high temperature (80 °C),[6a] the reaction performed in the presence of sodium acetate (1 equiv) at room temperature afforded a mixture of *cis*-, *trans*-, and *gem*-enynes and a consistent amount of an organometallic derivative, not yet identified. A convenient extension of the catalytic system **1**/

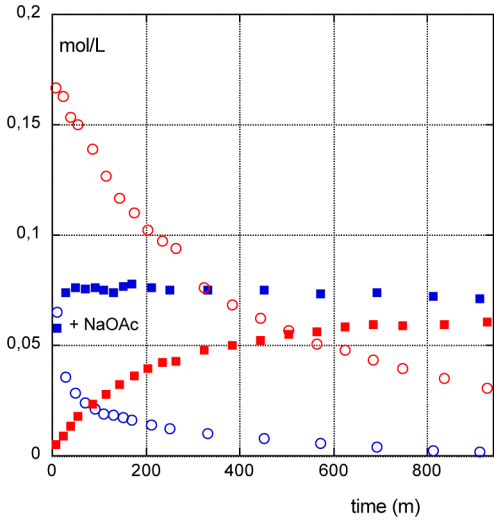

Figure 8. Dimerization of *p*-$CF_3C_6H_4C$≡CH (**4d**, 0.18 M, open circles) yielding **5a** (squares) catalyzed by **1** (red) or by **1**/NaOAc (blue), in CD_3CO_2H at 36 °C (**1**, 3.7 mol %; NaOAc, 1 equiv).

AcOH/NaOAc to aliphatic alkynes requires further investigation.

Formation and X-ray Structure of a 4-Alkynyl-η^3-dienyl Complex. This section explains that an organometallic ruthenium complex different from **1** and **3** is formed in the course of the reaction. Under preparative conditions, treatment of phenylacetylene (2.0 mmol) with complex **1** (2.5 mol %) and sodium acetate (0.5 equiv) for 24 h at room temperature afforded the enyne **5** (*trans*:*cis* = 98:2) in 73% isolated yield, after workup and purification by column chromatography (silica/DCM) (Scheme 2). Further elution with increasing polarity of the eluent (DCM/acetone 1/1) forced the separation of a dark red band, which was collected to give a red solid.

Scheme 2. Dimerization of PhC≡CH Promoted by 1/NaOAc in Acetic Acid

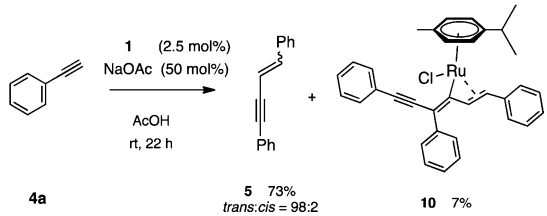

Spectroscopic and analytical data of this material were consistent with the structure of a η^3-hexa-1,3-dien-5-yn-3-yl complex, namely {Ru(η^6-*p*-cymene)Cl[η^3-(*E*,*Z*)-PhCH═CHC═C(Ph)C≡CPh]} (**10**), in which the organic ligand is derived from the formal coupling of three molecules of alkyne. Characteristic spectroscopic features of this complex are as follows: (i) the ν(C≡C) absorption band in the infrared at 2201 cm^{-1}, indicating that the triple bond is not bound to ruthenium, (ii) the hydrogen atoms of the *p*-cymene ligand exhibiting in the ^{1}H NMR spectrum four distinct doublets ($^3J_{H-H}$ = 5−6 Hz, 5.8−4.6 ppm), due to nonequivalency, (iii) the vinylic protons of the η^3-allyl group appearing as an AX system ($^3J_{H-H}$ = 11 Hz) within the same range, and (iv) the $^{13}C\{^1H\}$ NMR signal at 179.9 ppm corresponding to the C3

DOI: 10.1021/acs.organomet.7b00583
Organometallics 2017, 36, 3830−3840

carbon, σ-bound to ruthenium (Figures S22–S25 in the Supporting Information).

The formation of **10** accounts for 7 mol % of the starting alkyne and 50 mol % of ruthenium from complex **1**. When it was tested under catalytic conditions, complex **10** allowed for a sluggish conversion of phenylacetylene. It can therefore reenter the catalytic cycle, though with poor efficiency. One likely pathway for the formation of **10** involves π coordination of the enyne **5a** through the internal triple bond and insertion into an acetylide–ruthenium bond, as an effect of product competition for the catalytic species.[8] The molecule is analogous to the corresponding *m*-trifluoromethyl complex isolated after the one-pot desilylation/dimerization of *m*-$CF_3C_6H_4C{\equiv}CSiMe_3$ catalyzed by **1**. In that case, the reaction mixture contained excess sodium acetate due to quenching with acetic acid of the aqueous NaOH solution of the first step.[8]

A similar Cp* η^3-butadienyl complex, $[Ru(\eta^5\text{-}C_5Me_5)(PPh_3)\{\eta^3\text{-}PhCHCHC{=}CHPh(C{\equiv}CPh)\}]$ (**11**), featuring the same organic ligand as in **10**, was isolated in traces from the dimerization of **4a** promoted by a vinylidene complex in NEt_3/DCM.[22] Complex **11** was also prepared independently from the reaction of the vinylidene $[Ru(\eta^5\text{-}C_5Me_5)(PPh_3)Cl(C{=}CHPh)]$ with phenylacetylene in the presence of NaOMe or isolated as an impurity in the course of transformations of $[Ru(\eta^5\text{-}C_5Me_5)(PPh_3)_2(C{\equiv}CPh)]$.[23] Apparently, the formation of similar complexes with trimeric alkyne fragments is favored under different conditions.

The structure of complex **10** was determined by single-crystal X-ray diffraction analysis, from crystals obtained by slow evaporation of a chloroform solution. The ORTEP type representation of the complex is shown in Figure 9, and selected bonding data are collected in Table 6.

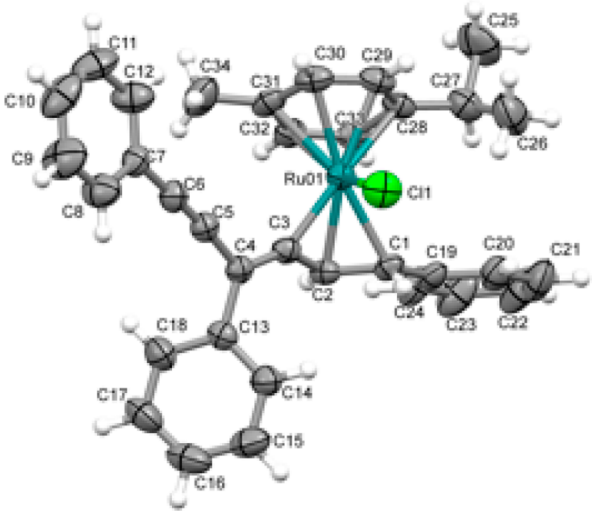

Figure 9. Molecular structure and atom-labeling scheme for $\{Ru(\eta^6\text{-}p\text{-cymene})Cl[\eta^3\text{-}(E,Z)\text{-}PhCH{=}CHC{=}C(Ph)\text{-}C{\equiv}CPh]\}$ (**10**). Hydrogen atoms have been omitted for clarity. Non-hydrogen atoms are represented by their 50% probability ellipsoids.

In the asymmetric unit the ruthenium atom is π-bonded to the benzene ring with an average Ru–C distance of 2.2315(3) Å (range 2.167(4)–2.299(3) Å), whereas the distance between the ruthenium atom and the centroid of the ring is 1.735 Å. These values are consistent with those for other Ru(II) η^6-arene complexes reported in the CSD database.[24] The diene fragment of the 1,3,6-triphenylhexa-3,5-dien-1-yne ligand is bound to Ru in η^3-*trans* coordination, in the same fashion as observed in the Cp* complex already mentioned.[22] This type of coordination is also found in other η^6-arene complexes with pentadienyl ligands.[25]

Catalytic Cycle for RAP Catalysis. The essential features of the catalytic cycle for the alkyne self-coupling can be regarded as being well understood for ruthenium(II) complexes, on the basis of several works available in the literature which include the study of single reactive steps and observation of intermediates.[1−9]

The proposed catalytic cycle shown in Scheme 3 refers to the specific conditions of the reaction promoted by **1** in acetic acid. On the basis of the previous comments, a complex such as **3** is assumed to be the catalytic species generated by interaction of **1** with $AcOH/AcO^-$.[26] Following π coordination of the alkyne on the metal (A), the acetate ligand acting as intramolecular base assists in C–H proton abstraction with formation of acetylide and a weakly bound molecule of acid (B). Ligand displacement by the second molecule of alkyne (C) followed by 1,2-H migration affords a vinylidene intermediate (D),[27] while the coupling step between the carbene and the acetylide carbon atoms yields a ruthenium enynyl complex (E).[28] Acetic acid then acts as a proton source for the release of the enyne product from ruthenium and generation of the acetate complex **3**.[20] Of course, alternatives to this picture are possible. For instance, the *endo* attack of the alkynyl group to the coordinated alkyne from C to E can occur, as proposed in the case of the dimerization of **4a** promoted by a cationic diruthenium complex.[4a]

Insights given by the current work into the catalytic cycle are worth comment. First of all, the formation of the enyne follows a first-order dependence on alkyne concentration, which is already apparent in the reactions in the presence of **1** alone but becomes clear with acetate cocatalysts.

This evidence implies the involvement of only one alkyne molecule in the rds, which thus should precede the formation of species C. Accordingly, the slowest step can be either the attack of ArC≡CH to complex **3** (**3** to A) or the intramolecular proton abstraction (A to B). The rate dependence on the electronic effect of the aryl substituents and the derived ρ value suggest that nucleophilic attack to the ruthenium center of complex **3** should benefit by increased electron density on the triple bond rather than proton abstraction, thus hinting at a preference for the former step as rate-limiting, which is also consistent with the observed negative entropy of activation in the reaction of **4a**. The formation of the enynyl complex from species D should also be favored by electron-donating substituents.[28c]

With regard to the reaction in presence of added acetate, the rapid formation of **3** and the catalytic activity exhibited by the preformed complex indicate that the effect is essentially intramolecular, although an intermolecular contribution cannot be excluded. For instance, the rate difference observed in the use of either lithium or sodium acetate may depend on the aggregation states of these acetate salts in acetic acid and different abilities to interact intermolecularly with the π-alkyne complex.

CONCLUSION

This work describes the transformation of the precursor dinuclear ruthenium complex **1** into the active catalytic species for the terminal alkyne dimerization reaction in a Brønsted acidic medium. Such formation and as a consequence the C–C

DOI: 10.1021/acs.organomet.7b00583
Organometallics 2017, 36, 3830–3840

Table 6. Selected Bond Lengths (Å) and Bond Angles (deg) for Complex 10

Bond Distances (Å)			
C(28)−Ru(01)	2.299(3)	C(31)−Ru(01)	2.281(3)
C(29)−Ru(01)	2.233(3)	C(32)−Ru(01)	2.186(3)
C(30)−Ru(01)	2.223(3)	C(33)−Ru(01)	2.167(3)
C(1)− Ru(01)	2.265(3)	C(2)−Ru(01)	2.172(3)
C(3)−Ru(01)	2.041(3)	C(1)−C(2)	1.403(4)
Cl1−Ru(01)	2.494(8)	C(5)−C(6)	1.188(4)
C(3)−C(04)	1.336(4)		
Bond Angles (deg)			
C(1)−C(2)−C(3)	118.60(3)	Cl(1)−Ru(1)−C(2)	100.93(7)
C(2)−C(3)−C(4)	140.12(3)	O(3)−Ru(01)−C(1)	84.05(7)
Cl(1)−Ru(1)−C(3)	84.80(8)		

Scheme 3. Proposed Catalytic Cycle for the Dimerization of Terminal Aryl Alkynes Initiated by [{RuCl(μ-Cl)(η^6-*p*-cymene)}$_2$] (1) in AcOH/AcO$^-$

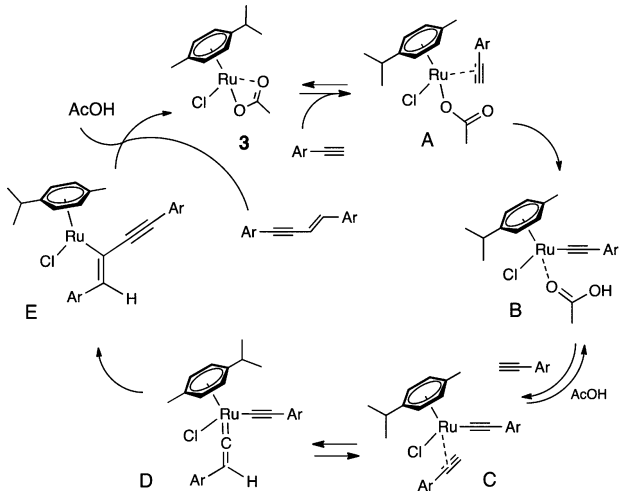

coupling process can be accelerated in presence of additive acetate salts, the intramolecular alkyne proton abstraction by acetate being a key step of the catalytic cycle. The derived catalytic system, on the basis of cooperative transition-metal and Brønsted acid catalysis, performs at room temperature with high stereoselectivity and short reaction times. Taking into account the use of commercially available materials, the combination **1**/AcOH/AcO$^-$ can be regarded as being among the most practical catalytic systems for the selective dimerization of terminal alkynes.

EXPERIMENTAL SECTION

General Procedures. All reagents and starting materials were obtained from commercial sources and used as received. Complex **3** was prepared as reported in the literature.[15] ^{1}H and ^{13}C{^{1}H} NMR spectra were recorded on a Bruker Avance II 300 spectrometer (300/75 MHz). Chemical shifts are reported in δ values relative to tetramethylsilane, with reference to internal solvent for ^{1}H ($CDCl_3$ at 7.27 ppm or CD_3CO_2H multiplet at 2.02 ppm) and for ^{13}C ($CDCl_3$ at 77.0 ppm) with coupling constants (J) given in Hz. FT infrared spectra were recorded on a Nicolet 510 spectrometer. GC-MS analyses were obtained on Agilent Technologies 6890N Network GC System equipped with a 5973 Network Mass Selective Detector. High-resolution ESI-TOF mass spectra were obtained on a Waters Micromass instrument. Analytical thin-layer chromatography (TLC) was performed on silica gel 60 F254 precoated glass or aluminum plates and preparative flash chromatography on a glass column packed with silica gel 60 (0.040−0.063 mm). The reactions were performed under an atmosphere of nitrogen using vacuum-line and standard Schlenk techniques. UV−vis kinetic measurements were performed on freshly prepared stock solutions of complex **1** and of sodium acetate in acetic acid using a Hewlett-Packard 8452A Diode Array Spectrophotometer coupled with a HI-TECH Scientific Pneumatic Drive Unit or a Varian Cary 300Bio instrument, equipped with thermostated cell holders. A typical procedure for ^{1}H NMR kinetic measurements is as follows. A 5 mm NMR tube was charged with weighted amounts of complex **1** and acetate salt, placed in a Kontes NMR manifold, and subjected to two vacuum−nitrogen cycles; first the solvent and then the liquid alkyne were added using a micro syringe. The tube was stoppered under nitrogen, and the mixture was shaken to result in a solution just before introduction into the NMR probe. Temperature calibration of the NMR probe was checked using a standard methanol solution. The sequential ^{1}H NMR spectra were analyzed by integration of the singlet signal due to the acetylenic proton of the substrate (3.8−3.6 ppm) and of the vinylic doublet of the *trans*-enyne ArCH=C*H*C≡CAr (6.5−6.0 ppm), with reference to the intensity of the solvent signals at 2.05 ppm. The stereoisomeric ratio was obtained by integration of the *trans* and *cis* vinylic doublets at the end of the runs, with similar values being observed in the course of the reaction. The reactions were generally followed for more than 90% formation of the *trans* dimer (near 4 half-lives) and yields determined upon addition of bibenzyl as an internal standard to the final reaction mixtures. Characterization data of enynes **5a**−**e** were reported elsewhere.[6a,8,9]

{Ru(η^6-*p*-cymene)Cl[η^3-(*E*,*Z*)-PhCH=CHC=C(Ph)C≡CPh]} (10). Complex **1** (30 mg, 0.50 mmol) and sodium acetate (9 mg, 0.11 mmol) were flushed with nitrogen in a Schlenk tube and then allowed to dissolve in acetic acid (3.0 mL), with stirring. Following addition of phenylacetylene (220 μL, 2.00 mmol), the tube was sealed with a rubber stopper, and the reaction was allowed to proceed for 22 h at room temperature. The initial dark red color of the solution changed slowly to dark brown. After removal of the solvent under vacuum (room temperature), the oily residue was purified by column chromatography with dichloromethane as eluent to obtain compound **5** (149 mg, yield 72%) and complex **10** (29 mg, 7%). FT-IR (film on KBr): ν 3052, 2963, 2925, 2870, 2200 (−C≡C−), 1753, 1677, 1595, 1511, 1490, 1468, 1443, 1382, 1321, 1258, 1216, 1156, 1070, 1033, 910, 845, 790, 756, 692, 665, 652, 611, 598, 569, 548, 527, 512, 487, 441.13 cm^{-1}. ^{1}H NMR (300 MHz, $CDCl_3$): δ 7.77 (d, $^3J_{H-H}$ = 8 Hz, 2H, PhH), 7.63 (d, $^3J_{H-H}$ = 8 Hz, 2H, PhH), 7.50 (d, $^3J_{H-H}$ = 7 Hz, 2H, PhH), 7.43−7.31 (m, 8H, PhH), 7.18 (t, $^3J_{H-H}$ = 7 Hz, 1H, PhH), 5.78 (d, $^3J_{H-H}$ = 5.1 Hz, 1H, *p*-cymene CH), 5.26 (dd, $^3J_{H-H}$ = 6.1 Hz, $^4J_{H-H}$ = 1.2 Hz, 1H, *p*-cymene CH), 5.20 (d, $^3J_{H-H}$ = 5.9 Hz, 1H, *p*-cymene CH), 5.1 (d, $^3J_{H-H}$ = 11.2 Hz, 1H, vinyl CH), 4.74 (d, $^3J_{H-H}$ = 11.3 Hz, 1H, vinyl CH), 4.61 (d, $^3J_{H-H}$ = 4.9 Hz, 1H, *p*-cymene CH), 2.55 (eptuplet, $^3J_{H-H}$ = 7 Hz, 1H, C*H*Me$_2$), 2.07 (s, 3H, Me), 1.19 (d, $^3J_{H-H}$ = 7 Hz, 3H, CH*Me*), 1.13 (d, $^3J_{H-H}$ = 7 Hz, 3H, CH*Me*) ppm. ^{13}C{^{1}H} NMR (75 MHz, $CDCl_3$): δ 179.88 (Ru−C), 140.75, 137.13, 131.67, 128.9, 128.32, 128.06, 127.56, 127.05, 126.37, 126.13, 126.02, 115.14, 114.73, 101.13, 92.29, 91.55, 90.47, 87.33, 82.66, 77.14 ($CDCl_3$), 63.38, 30.65, 23.28, 21.63, 18.24 ppm. MS-ESI (M = $C_{34}H_{31}ClRu$, 576.116): 541.1616 (cluster; calcd for $C_{34}H_{31}Ru$

DOI: 10.1021/acs.organomet.7b00583
Organometallics 2017, 36, 3830−3840

541.1469; M − Cl); 582.160 (cluster, calcd for $C_{34}H_{31}RuK$ 582.112; M − Cl + K); 599.120 (cluster, calcd for $C_{36}H_{34}O_2Ru$ 599.161; M − Cl + AcO); 1175.1848 (cluster, calcd for $C_{70}H_{65}ClO_2Ru_2$ 1175.279; 2 M − Cl + OAc).

X-ray Crystallography. The diffraction data from a selected single crystal were collected at room temperature on an Oxford Diffraction Xcalibur Gemini S diffractometer using Mo Kα radiation (λ = 0.71073 Å). The data were processed with CrysAlis software, and empirical absorption correction using spherical harmonics were implemented in the SCALE3 ABSPACK scaling algorithm.[29] The crystallographic data, the data collection parameters, and the refinement parameters for compound **10** are summarized in the Supporting Information. The crystal structure was solved by direct methods using SHELXT and refined by full-matrix least-squares calculations against F^2 using SHELXL.[30] All non-hydrogen atoms were refined with anisotropic displacement parameters. All aromatic C−H atoms were included in their calculated positions and treated as riding atoms: C−H = 0.93 Å for aromatic CH with $U_{iso}(H) = 1.2 \times U_{eq}(C)$. The figures were produced using MERCURY.[31] The software used for the preparation of the materials for publication was WinGX[32] and PLATON.[33]

■ ASSOCIATED CONTENT

Supporting Information

The Supporting Information is available free of charge on the ACS Publications website at DOI: 10.1021/acs.organomet.7b00583.

UV−vis spectra of compounds **1**, **3**, and **5**, kinetic plots for the reaction of **1** in acetic acid and with sodium acetate, selected reaction profiles and kinetic fits for the dimerization reaction, ^1H and $^{13}C\{^1H\}$ NMR, FT-IR, and MS-ESI spectra, and crystal data, data collection and structure refinement details for complex **10** (PDF)

Accession Codes

CCDC 1545810 contains the supplementary crystallographic data for this paper. These data can be obtained free of charge via www.ccdc.cam.ac.uk/data_request/cif, or by emailing data_request@ccdc.cam.ac.uk, or by contacting The Cambridge Crystallographic Data Centre, 12 Union Road, Cambridge CB2 1EZ, UK; fax: +44 1223 336033.

■ AUTHOR INFORMATION

Corresponding Author

*E-mail for M.B.: mauro.bassetti@cnr.it.

ORCID

Riccardo Salvio: 0000-0003-0398-8408

Francisco Juliá-Hernández: 0000-0001-5311-0957

Mauro Bassetti: 0000-0002-8163-3234

Notes

The authors declare no competing financial interest.

■ ACKNOWLEDGMENTS

The research was performed under the joint activity IMC-Dipartimento di Chimica. Projects "Sistemi catalitici innovativi per lo sviluppo di processi sostenibili" (CNR_DCM.AD001.212) and Ateneo−La Sapienza 2016 (RM116154C9CFDE3B) are acknowledged for financial support. F.J.-H. thanks the Fundación Séneca (03059/PI/05), Región de Murcia (ES), for a predoctoral fellowship at CNR-IMC. S.G.-G. and R.M.-M. acknowledge the financial support provided by the MINECO, Project MAT2013-40950-R, ERDF funding, and Project MAT2016-78155-C2-1-R". Dedicated to Prof. Peter Maitlis who inspired me to search for the mechanism of the catalyst action.

■ REFERENCES

(1) Reviews: (a) García-Garrído, S. E. Catalytic Dimerization of Alkynes. In *Modern Alkyne Chemistry: Catalytic and Atom-Economic Transformations*; Trost, B. M., Li, C.-J., Eds.; Wiley: Hoboken, NJ, 2015; pp 299−334. (b) Trost, B. M.; McClory, A. *Chem. - Asian J.* **2008**, *3*, 164−194. (c) Bustelo, E.; Dixneuf, P. H. In *Handbook of C-H Transformations*; Dyker, G., Ed.; Wiley-VCH: Weinheim, Germany, 2005; Vol. *1*, Chapter II. (d) Drozdzak, R.; Allaert, B.; Ledoux, N.; Dragutan, I.; Dragutan, V.; Verpoort, F. *Adv. Synth. Catal.* **2005**, *347*, 1721−1743. (e) Wakatsuki, Y. *J. Organomet. Chem.* **2004**, *689*, 4092−4109.

(2) Selected articles: (a) Żak, P.; Bołt, M.; Lorkowski, J.; Kubicki, M.; Pietraszuk, C. *ChemCatChem* **2017**, DOI: 10.1002/cctc.201700580. (b) Liang, Q.; Osten, K. M.; Song, D. *Angew. Chem., Int. Ed.* **2017**, *56*, 6317−6320. (c) Rivada-Wheelaghan, O.; Chakraborty, S.; Shimon, L. J. W.; Ben-David, Y.; Milstein, D. *Angew. Chem.* **2016**, *128*, 7056. (d) Pell, C. J.; Ozerov, O. G. *ACS Catal.* **2014**, *4*, 3470−3480. (e) Midya, G. C.; Paladhi, S.; Dhara, K.; Dash, J. *Chem. Commun.* **2011**, *47*, 6698−670. (f) Katagiri, T.; Tsurugi, H.; Satoh, T.; Miura, M. *Chem. Commun.* **2008**, 3405−3407. (g) Ge, S.; Norambuena, V. F. Q.; Hessen, B. *Organometallics* **2007**, *26*, 6508−6510. (h) Weng, W.; Guo, C.; Çelenligin-Çetin, R.; Foxman, B. M.; Ozerov, O. V. *Chem. Commun.* **2006**, 197−199. (i) Hirabayashi, T.; Sakaguchi, S.; Ishii, Y. *Adv. Synth. Catal.* **2005**, *347*, 872−876. (l) Ogoshi, S.; Ueta, M.; Oka, M.; Kurosawa, H. *Chem. Commun.* **2004**, 2732−2733. (m) Nishiura, M.; Hou, Z.; Wakatsuki, Y.; Yamaki, T.; Miyamoto, T. *J. Am. Chem. Soc.* **2003**, *125*, 1184−1185.

(3) (a) Pasquini, C.; Fratoddi, I.; Bassetti, M. *Eur. J. Org. Chem.* **2009**, *2009*, 5224−5231. (b) Liu, Y.; Nishiura, M.; Wang, Y.; Hou, Z. *J. Am. Chem. Soc.* **2006**, *128*, 5592−5593. (c) Norambuena, V. F. Q. Ph.D. Dissertation, University of Groningen, 2006; Chapter 6. (d) Katayama, H.; Nakayama, M.; Nakano, T.; Wada, C.; Akamatsu, K.; Ozawa, F. *Macromolecules* **2004**, *37*, 13−17.

(4) (a) Kiyota, S.; Soeta, H.; Komine, N.; Komiya, S.; Hirano, M. *J. Mol. Catal. A: Chem.* **2017**, *426*, 419−428. (b) Chen, C.-R.; Lin, Y.-C. *Organometallics* **2014**, *33*, 6408−6412. (c) Prades, A.; Viciano, M.; Sanaú, M.; Peris, E. *Organometallics* **2008**, *27*, 4254−4259. (d) Katayama, H.; Yari, H.; Tanaka, M.; Ozawa, F. *Chem. Commun.* **2005**, 4336−4338. (e) Baratta, W.; Herrmann, W. A.; Rigo, P.; Schwarz, J. *J. Organomet. Chem.* **2000**, *593*−*594*, 489−493. (f) Yi, C. S.; Liu, N. *Organometallics* **1996**, *15*, 3968−3971.

(5) (a) Chen, C.-K.; Tong, H.-C.; Chen Hsu, C.-Y.; Lee, C.-Y.; Fong, Y. H.; Chuang, Y.-S.; Lo, Y.-H.; Lin, Y.-C.; Wang, Y. *Organometallics* **2009**, *28*, 3358−3368. (b) Novak, P.; Kotora, M. *Collect. Czech. Chem. Commun.* **2009**, *74*, 433−442. (c) Chen, X.; Xue, P.; Sung, H. H. Y.; Williams, I. D.; Peruzzini, M.; Bianchini, C.; Jia, G. *Organometallics* **2005**, *24*, 4330−4332.

(6) (a) Bassetti, M.; Pasquini, C.; Raneri, A.; Rosato, D. *J. Org. Chem.* **2007**, *72*, 4558−4561. (b) Donoli, A.; Bisello, A.; Cardena, R.; Ceccon, A.; Bassetti, M.; D'Annibale, A.; Pasquini, C.; Raneri, A.; Santi, S. *Inorg. Chim. Acta* **2011**, *374*, 442−446.

(7) Pasquini, C.; Fratoddi, I.; Capitani, D.; Mannina, L.; Bassetti, M. *J. Org. Chem.* **2008**, *73*, 3892−3899.

(8) Pasquini, C.; Bassetti, M. *Adv. Synth. Catal.* **2010**, *352*, 2405−2410.

(9) Coniglio, A.; Bassetti, M.; García-Garrido, S. E.; Gimeno, J. *Adv. Synth. Catal.* **2012**, *354*, 148−158.

(10) (a) Ackermann, L. *Org. Process Res. Dev.* **2015**, *19*, 260−269. (b) Li, B.; Dixneuf, P. H. *Chem. Soc. Rev.* **2013**, *42*, 5744−5767. (c) Ackermann, L. *Chem. Rev.* **2011**, *111*, 1315−1345. (d) Ackermann, L.; Vicente, R.; Althammer, A. *Org. Lett.* **2008**, *10*, 2299−2302. (e) García-Cuadrado, D.; de Mendoza, P.; Braga, A. A. C.; Maseras, F.; Echavarren, A. M. *J. Am. Chem. Soc.* **2007**, *129*, 6880−6886. (f) Alberico, D.; Scott, M. E.; Lautens, M. *Chem. Rev.* **2007**, *107*, 174−238.

(11) Ackermann, L. *Acc. Chem. Res.* **2014**, *47*, 281−295.

(12) Johnson, D. G.; Lynan, J. M.; Slattery, J. M.; Welby, C. E. *Dalton Trans* **2010**, *39*, 10432−10441.

(13) Zatolochnaya, O. V.; Goordev, E. G.; Jahier, C.; Ananikov, V. P.; Gevorgyan, V. *Chem. - Eur. J.* **2014**, *20*, 9578−9588.
(14) (a) Cook, J.; Hamlin, J. E.; Nutton, A.; Maitlis, P. M. *J. Chem. Soc., Dalton Trans.* **1981**, 2342−2352. (b) Tocher, D. A.; Gould, R. O.; Stephenson, T. A.; Bennett, M. A.; Ennett, J. P.; Matheson, T. W.; Sawyer, L.; Shah, V. K. *J. Chem. Soc., Dalton Trans.* **1983**, 1571−1581.
(15) (a) Davies, D. L.; Al-Duaij, O.; Fawcett, J.; Giardiello, M.; Hilton, S. T.; Russell, D. R. *Dalton Trans.* **2003**, 4132−4138. (b) Melchart, M.; Habtemariam, A.; Parsons, S.; Moggach, S. A.; Sadler, P. J. *Inorg. Chim. Acta* **2006**, *359*, 3020−3028.
(16) Eigen, M.; Wilkins, R. G. The Kinetics and Mechanism of Formation of Metal Complexes, Mechanism of Inorganic Reactions. *Adv. Chem. Ser.* **1965**, *49*, 55−80.
(17) (a) Bennett, M. A.; Ennett, J. P. *Organometallics* **1984**, *3*, 1365−1374. (b) Daguenet, C.; Scopelliti, R.; Dyson, P. J. *Organometallics* **2004**, *23*, 4849−4857. (c) Chen, H.; Li, S. *Organometallics* **2005**, *24*, 872−884. (d) Martínez-Alonso, M.; Busto, N.; Jalón, F. A.; Manzano, B. R.; Leal, J. M.; Rodríguez, A. M.; García, B.; Espino, G. *Inorg. Chem.* **2014**, *53*, 11274−11288.
(18) (a) Halpern, J.; James, B. R. *Can. J. Chem.* **1966**, *44*, 495−500. (b) Monteiro, M. C. R.; Nascimento, F. B.; Valle, E. M. A.; Ellena, J.; Castellano, E. E.; Batista, A. A.; Machado, S. P. *J. Braz. Chem. Soc.* **2010**, *21*, 1992−1999.
(19) Shields, G. C.; Seybold, P. G. *Computational Approaches for the Prediction of pKa Values*; CRC Press: Boca Raton, FL, 2014.
(20) (a) Bianchini, C.; Frediani, P.; Masi, D.; Peruzzini, M.; Zanobini, F. *Organometallics* **1994**, *13*, 4616−4632. (b) Melis, K.; De Vos, D.; Jacobs, P.; Verpoort, F. *J. Organomet. Chem.* **2002**, *659*, 159−164. (c) Melis, K.; Opstal, T.; Verpoort, F. *Eur. J. Org. Chem.* **2002**, *2002*, 3779−3784. (d) Jiménez-Tenorio, M.; Puerta, M. C.; Valerga, P. *Organometallics* **2009**, *28*, 2787−2798.
(21) Hansch, C.; Leo, A.; Taft, R. W. *Chem. Rev.* **1991**, *91*, 165−195.
(22) Yi, C. S.; Liu, N.; Rheingold, A. L.; Liable-Sands, L. M. *Organometallics* **1997**, *16*, 3910−3913.
(23) (a) Bruce, M. I.; Hall, B. C.; Skelton, B. W.; White, A. H.; Zaitseva, N. N. *J. Chem. Soc., Dalton Trans.* **2000**, 2279−2286. (b) Bruce, M. I.; Skelton, B. W.; White, A. H.; Zaitseva, N. N. *J. Chem. Soc., Dalton Trans.* **2001**, 3627−3633.
(24) CSD database version 5.37 (for 215 hits found Ru−C mean distance 2.220(3) Å and centroid−Ru mean distance 1.1717(3) Å). Allen, F. H. *Acta Crystallogr., Sect. B: Struct. Sci.* **2002**, *58*, 380−388.10.1107/S0108768102003890
(25) Ramirez-Monroy, A.; Paz-Sandoval, M. A.; Ferguson, M. J.; Stryker, J. M. *Organometallics* **2007**, *26*, 5010−5024.
(26) Other assumptions in the proposed catalytic cycle include the retention of coordinated *p*-cymene, due to the mild reaction conditions, and of one chloride ion. However, transient dissociation of this anion during the cycle cannot be excluded.
(27) Welby, C. E.; Eschemann, T. O.; Unsworth, C. A.; Smith, E. J.; Thatcher, R. J.; Whitwood, A. C.; Lynam, J. M. *Eur. J. Inorg. Chem.* **2012**, *2012*, 1493−1506. (a) Bassetti, M.; Cadierno, V.; Gimeno, J.; Pasquini, C. *Organometallics* **2008**, *27*, 5009−5016.
(28) (a) Albertin, G.; Antoniutti, S.; Bordignon, E.; Cazzaro, F.; Ianelli, S.; Pelizzi, G. *Organometallics* **1995**, *14*, 4114. (b) Bassetti, M.; Marini, S.; Díez, J.; Gamasa, M. P.; Gimeno, J.; Rodrígez-Álvarez, Y.; García-Granda, S. *Organometallics* **2002**, *21*, 4815−4822. (c) Eaves, S. G.; Yufit, D. S.; Skelton, B. W.; Lynam, J. M.; Low, P. J. *Dalton Trans.* **2015**, *44*, 21016−21024. (d) Martínez de Salinas, S.; Díez, J.; Falvello, L. R.; González, J.; Gamasa, M. P.; Lastra, E. *Organometallics* **2016**, *35*, 2793−2805.
(29) *CrysAlis PRO, CrysAlis CCD and CrysAlis RED*; Oxford Diffraction Ltd, Yarnton, Oxfordshire, England, 2010.
(30) Sheldrick, G. M. *Acta Crystallogr., Sect. A: Found. Crystallogr.* **2008**, *64*, 112−122.
(31) Macrae, C. F.; Bruno, I. J.; Chisholm, J. A.; Edgington, P. R.; McCabe, P.; Pidcock, E.; Rodríguez-Monge, L.; Taylor, R.; van de Streek, J.; Wood, P. A. *J. Appl. Crystallogr.* **2008**, *41*, 466−470.
(32) Farrugia, L. J. *J. Appl. Crystallogr.* **1999**, *32*, 837−838.
(33) Spek, A. L. *J. Appl. Crystallogr.* **2003**, *36*, 7−13.

DOI: 10.1021/acs.organomet.7b00583
Organometallics 2017, 36, 3830−3840